DNA repair in plant mitochondria - A complete base excision repair pathway in potato tuber mitochondria

Ferrando, Beatriz; de Matos Furlanetto, Ana Luiza Dorigan; Gredilla, Ricardo; Havelund, Jesper F; Hebelstrup, Kim H; Møller, Ian Max; Stevnsner, Tinna

Published in:
Physiologia Plantarum

DOI:
10.1111/ppl.12801

Publication date:
2019

Document version:
Accepted manuscript

Citation for pulished version (APA):
Ferrando, B., de Matos Furlanetto, A. L. D., Gredilla, R., Havelund, J. F., Hebelstrup, K. H., Møller, I. M., & Stevnsner, T. (2019). DNA repair in plant mitochondria - A complete base excision repair pathway in potato tuber mitochondria. *Physiologia Plantarum*, *166*(2), 494-512. https://doi.org/10.1111/ppl.12801

DNA repair in plant mitochondria

– A complete base excision repair pathway in potato tuber mitochondria

Beatriz Ferrando[a], Ana Luiza Dorigan de Matos Furlanetto[b], Ricardo Gredilla[a,c], Jesper F. Havelund[d], Kim H. Hebelstrup[e], Ian Max Møller[e,*] and Tinna Stevnsner[a,*]

[a]Department of Molecular Biology and Genetics, Aarhus University, C.F. Møllers Allé 3, DK-8000 Aarhus C, Denmark

[b]Department of Biochemistry and Molecular Biology, Life sciences sector, Federal University of Paraná, CP 19046, CEP 81531-990 Curitiba-PR, Brazil

[c]Department of Physiology, Faculty of Medicine, Complutense University, Plaza Ramon y Cajal s/n, 28040, Madrid, Spain

[d]Department of Biochemistry and Molecular Biology, University of Southern Denmark, Campusvej 55, DK-5230 Odense M, Denmark

[e]Department of Molecular Biology and Genetics, Aarhus University, Forsøgsvej 1, DK-4200 Slagelse, Denmark

Correspondence

Corresponding authors,

e-mail: ian.max.moller@mbg.au.dk, tvs@mbg.au.dk

Mitochondria are one of the major sites of reactive oxygen species (ROS) production in the plant cell. ROS can damage DNA, and this damage is in many organisms mainly repaired by the base excision repair (BER) pathway. We know very little about DNA repair in plants especially in the mitochondria. Combining proteomics, bioinformatics, Western blot and enzyme assays we here demonstrate that the complete BER pathway is found in mitochondria isolated from potato (*Solanum tubersosum*) tubers. The enzyme activities of three DNA glycosylases and an apurinic/apyrimidinic (AP) endonuclease were characterized with respect to Mg^{2+} dependence and, in the case of the AP endonuclease, temperature sensitivity. Evidence for the presence of the DNA polymerase and the DNA ligase, which complete the repair pathway by replacing the excised base and closing the gap, was also obtained. We tested the effect of oxidative stress on the mitochondrial BER pathway by incubating potato tubers under hypoxia. Protein carbonylation increased significantly in hypoxic tuber mitochondria indicative of increased oxidative stress. The activity of two BER enzymes increased significantly in response to this oxidative stress consistent with the role of the BER pathway in the repair of oxidative damage to mtDNA.

This article has been accepted for publication and undergone full peer review but has not been through the copyediting, typesetting, pagination and proofreading process, which may lead to differences between this version and the Version of Record. Please cite this article as doi: 10.1111/ppl.12801

Abbreviations – APE, apurinic/apyrimidinic endonuclease; BER, base excision repair; MLM, mouse liver mitochondria; Neil1/2, Neil1/2 glycosylase; POM, potato mitochondria; ROS, reactive oxygen species; UNG, uracil DNA glycosylase, OGG1,8-oxoguanine-DNA glycosylase.

Introduction

DNA can be damaged in different ways, many of which can lead to mutations (Grollman and Moriya 1993, Kavli et al. 2007, Liu et al. 2016). It is therefore essential for the organism to be able to repair DNA damage. In mammalian cells different DNA repair pathways are present in both the nucleus and the mitochondria (Jeppesen et al. 2011). DNA repair is even more complex in plant cells as they contain a second DNA-containing organelle, the chloroplast (Oldenburg and Bendich 2015).

One of the major sources of DNA damage is reactive oxygen species (ROS), which can modify DNA in a number of different ways where the major one is the formation of 8-oxoguanine (8-oxoG) (Maynard et al. 2009). As chloroplasts and mitochondria are major sites of ROS production in the plant cell (Maxwell et al. 1999, Møller 2001, Foyer and Noctor 2003), they need to have efficient systems for repairing their DNA especially with respect to oxidative DNA damage. Mammalian mitochondria contain several different repair pathways (Kazak et al. 2012); but the BER pathway repairs the majority of the DNA lesions produced by ROS. This pathway primarily corrects small base modifications caused by deamination, alkylation, and oxidation (Kim and Wilson 2012). It can proceed as either short-patch (exchange of a single nucleotide) or long-patch (repair tract of two or more nucleotides). The process takes place in five steps as shown in Fig. 1. Briefly, the first step is catalyzed by a specific DNA glycosylase with a well-defined substrate specificity, which recognizes the modified base, and cleaves the N-glycosidic bond creating an apurinic/apyrimidinic (AP) site. The glycosylases can be divided into (1) monofunctional glycosylases, which include uracil glycosylase (UNG) that removes non-oxidative base damage, due to deamination or alkylation, and (2) bifunctional glycosylases, which include e.g. Neil1/2 and OGG1 that excise oxidized DNA bases and in addition to the cleavage activity described above, also possess AP lyase activity. The latter allows the cleavage of the DNA backbone and generation of a 3'-deoxyribose phosphate (dRP) at the AP site. The AP site is then processed by an AP endonuclease (or in some cases by polynucleotide kinase/phosphatase (PNKP)), which creates a strand break with a 3'-hydroxyl end and a 5'(dRP) residue. The gap is then filled by an mtDNA polymerase, generally considered to be DNA polymerase γ (Polγ) in mammals, but recently DNA polymerase β (Polβγ has also been reported to be involved, not only in nuclear, but also in mitochondrial BER (Saxowsky et al. 2003, Sykora et al. 2017, Prasad et al. 2017). Recently, Trasvina-Arenas et al. (2018) identified two DNA polymerases in *Arabidopsis thaliana* (Arabidopsis), which may play a role in short-patch and long-patch BER, respectively. In long-patch BER the flap that is created is removed by a flap endonuclease. Finally, the nick is sealed by a DNA ligase.

Unlike mtDNA in mammals, plant mtDNA has accumulated very few point mutations during evolution (Palmer and Herbon 1988, Lynch et al. 2006, Lynch 2007) suggesting that their DNA repair systems are very efficient. However, we know very little about the DNA repair systems in plant mitochondria (Gualberto and Newton 2017). Uracil-DNA glycosylase activity was detected in vitro in

mitochondria of *Zea mays* seedlings (Bensen and Warner 1987). Both uracil and AP endonuclease activity were characterized in vitro and in organelle assays with Arabidopsis and *Solanum tuberosum* mitochondria (Boesch et al. 2009). A number of enzymes have been predicted to be involved in mitochondrial BER in Arabidopsis as reviewed in (Gualberto and Newton 2017).

In the present study, we have identified the main components of the BER pathway in potato tuber mitochondria (POM) by using a combination of immuno-detection, enzymatic assays, proteomics and bioinformatics. We have further characterized the response of the pathway to in vivo long-term hypoxia to induce oxidative stress. For some of the analyses we made comparisons to mouse liver mitochondria (MLM), which previously have been carefully characterized with regard to the BER pathway.

Materials and methods

Preparation and storage of mitochondria from potato tubers and mouse liver

Highly purified and functional mitochondria were isolated from potato (*Solanum tuberosum* L. cv. *Folva*) tubers stored at 5-10°C by the method of Havelund (2014). MLM were isolated as described by Gredilla and Stevnsner (2012).
The mitochondrial protein concentration was estimated by Bradford (1976) protein assay.

Proteomic profiling of potato tuber mitochondria

To identify as many low-abundance proteins as possible we performed a proteomic profiling using a more sensitive method than in previous studies (Supplementary data 7).

Using this procedure more than 2600 different proteins were identified, out of which about 1600 proteins were found in at least two samples. Only proteins related to the BER pathway are documented here (Table S2). The full proteome will be published elsewhere.

NCBI databases

The LC-MS data was searched against a database of *S. tuberosum* entries downloaded from NCBI in February 2014. When manually searching for the BER proteins (Supplementary data 1-6), a newer database of *S. tuberosum* entries from January 2017 was used.

Hypoxia treatment

Potato tubers stored in darkness at room temperature (25°C) for 3 days were incubated in a closed container under hypoxia (0.1/99.9% oxygen/nitrogen) for 48 h followed by normoxia for 24 h, all at

room temperature (22-24°C). Control sample was kept in darkness under normoxic conditions at room temperature.

Oligonucleotides

All oligonucleotides were purchased from DNA Technology and were radioactively labeled at the 5'-end using γ-[^{32}P]ATP (Perkin-Elmer) and T4 polynucleotide kinase (PNK) (Thermo Scientific, Roskilde, Denmark). Mixtures of 100 µg oligonucleotides containing the DNA lesion (Table 1), 20 units of T4 PNK, PNK forward buffer A and 12.3 MBq γ-[^{32}P]ATP were incubated for 90 min at 37°C. Labeling was terminated by adding EDTA to a final concentration of 10 mM. Unincorporated γ-[^{32}P]ATP was removed using G50 Microspin columns. KCl was added to the eluate to a final concentration of 50 mM together with the corresponding complementary strand and the two were annealed by heating to 90°C followed by gradual and slow cooling of the reaction to room temperature.

Mitochondrial DNA glycosylase activities

Mitochondrial activity of various DNA glycosylases was measured after mitochondrial permeabilization in the presence of 0.05 % Triton X-100 and 0.3 M KCl for 2 min on ice. Incision assays were performed by incubating different protein amounts (as indicated) of purified MLM at 37 °C and POM at 25°C in a 20 µl reaction volume in a reaction buffer containing 20 mM HEPES/KOH (pH 7.6), 75 mM KCl, 5% (v/v) glycerol, 2 mM DTT, 0.1 mg ml^{-1} BSA, 5 mM EDTA and, 7.5 mM dNTPs (glycosylase incision assay condition). For incision assay of 5-OH-dU and dU, 36 fmol of the corresponding duplexed ^{32}P-end-labeled DNA substrate (Table 1) were used in the reactions with different concentrations of $MgCl_2$ during 180 min (if not otherwise indicated). For incision of 8-Oxo-dG 80 fmol of substrate (Table 1) was used with 10 mM $MgCl_2$ in POM and 1 mM $MgCl_2$ in MLM and the incubation time was 180 min. Reactions were stopped by adding 0.4 % SDS and 0.2 µg µl^{-1} of proteinase K, and by 30 min incubation at 55°C. Finally, the samples were mixed with 20 µl of formamide dye loading buffer (80% formamide, 10 mM EDTA, 1 mg ml^{-1} xylene cyanol FF and, 1 mg/mL Bromophenol Blue) and heated for 2 min at 90°C. It is our experience that this procedure leads to cleavage of the DNA backbone at abasic sites, which may not have been cleaved already by the AP-lyase activity of the glycosylase. Thus, the observed amount of product shown in Figs 2-4 reflects the glycosylase activity and not the lyase activity of the bifunctional glycosylases. Substrates and products were separated using a 20% denaturing polyacrylamide gel, and the radioactively labeled DNA was visualized using Storage Phosphor screens (Amersham Bioscience), scanned using a Personal Molecular ImagerTM and quantified using Image Lab software (Bio-Rad). DNA enzyme activities were calculated as the number of pixels in the product band relative to the total pixels of both bands. If

a product band appeared in the absence of mitochondrial extract, this background was subtracted from the activity in the other samples.

To identify nonspecific cleavage, all conditions measuring DNA glycosylase activities were also performed with an identical oligonucleotide but without the modified base. No nonspecific cleavage was found in any of these control experiments (data not shown).

Mitochondrial AP endonuclease activity

The activity of AP endonuclease in mitochondria from mouse liver and tuber potato was determined by incision assay with an AP endonuclease specific substrate. After permeabilization in the presence of 0.05% (w/v) Triton X-100 and 0.3 M KCl for 2 min, mitochondria were incubated in a 20 µl reaction containing 36 fmol of the ^{32}P end-labeled DNA substrate containing the THF (Table 1), 20 mM HEPES/KOH (pH 7.6), 75 mM KCl, 5% glycerol, 5 mM DTT (APE1 incision assay condition), and different concentrations of divalent cations, chelating agents and increasing protein amounts of purified MLM or POM (as indicated), for 30 min at 37°C for MLM and 25°C for POM (if not otherwise indicated). Reactions were terminated by addition of 0.4 % SDS and 0.2 µg µl^{-1} of proteinase K, followed by 30 min incubation at 55°C. Finally, the samples were mixed with 20 µl of formamide dye loading buffer (80% formamide, 10 mM EDTA, 1 mg ml^{-1} xylene cyanol FF and, 1 mg ml^{-1} Bromophenol Blue) and heated for 2 min at 90°C. Substrates and products were separated on a 20% denaturing polyacrylamide gel, and the radioactively labeled DNA was visualized using Storage Phosphor screens (Amersham Bioscience), scanned using a Personal Molecular ImagerTM and quantified using Image Lab software (Bio-Rad). AP endonuclease activities were calculated as the amount of pixels in the product band relative to the total number of pixels in both bands. If a product band appeared in the absence of mitochondria, this background was subtracted from the activity in the other samples.

To identify potential nonspecific activities, all conditions measuring APE1-like activities were also performed with an identical oligonucleotide, but without the modified base. No nonspecific activities were found in any of these control experiments (data not shown).

DNA polymerase and DNA ligase activity

Repair synthesis was measured by using a non-labeled 60 base-pair hairpin loop oligonucleotide containing d-Uracil (Table 1). Reactions for both MLM and POM contained 40 mM HEPES, pH 7.8, 0.1 mM EDTA, 0.2 mg ml^{-1} BSA, 1 mM DTT, 40 mM phosphocreatine, 100 µg ml^{-1} phosphocreatine kinase, 2 mM ATP, 20 µM dNTPs, 4 µCi ^{32}P-dCTP, and 100 ng double-stranded oligonucleotide, adding 50 mM KCl and 3% glycerol for MLM, and 150 mM KCl, 10% glycerol and 4 mM $MgCl_2$ for

POM, in 50 µl. 90 µg of mitochondria fractions were added, and reaction mixtures were incubated at 37°C for MLM and at 25°C for POM for 3 h. The reactions were terminated by adding 12.5 µg of proteinase K (PNK) and 2.5 µl of 10% SDS and incubating at 55°C for 30 min. DNA was precipitated by addition of 1 µg glycogen, 4 µl of 11 M ammonium acetate, 60 µl of ethanol and overnight incubation at −20°C. DNA was centrifuged, dried and resuspended in 20 µl of formamide loading dye (80% formamide, 10 mM EDTA, 1 mg ml^{-1} xylene cyanol FF, and 1 mg ml^{-1} bromophenol blue) and loaded on a 20% denaturing polyacrylamide gel. The incorporated radioactively labeled dCTP was visualized using Storage Phosphor screens (Amersham Bioscience), scanned using a Personal Molecular ImagerTM and quantified using Image Lab software (Bio-Rad).

DNA melting temperature

For assessment of DNA melting temperature (Tm) reaction mixtures contained 250 nM annealed, unlabeled THF DNA, 40 mM HEPES/KOH (pH 7.6), 2 mM DTT, 5% glycerol, and 75 mM KCl and 1× SyBR green (Invitrogen), were incubated with different divalent cations and chelating agents (as indicated). Reactions were analyzed using a Stratagene Mx3000P qPCR analyzer determining a dissociation curve from 37 to 95°C.

Protein sequence alignment

Basic Local Alignment Search Tool (BLASTP 2.5.1) (Altschul 1997) was used to search the putative sequence alignment of *S. tuberosum* BER enzymes, and to compare with its mouse and human homologues.

SDS-PAGE and Western Blotting

Mitochondrial samples (40 µg of proteins) were separated on 4-12% NuPAGE Novex® Bis-Tris gels (invitrogen). Proteins were then transferred to PVDF membranes (Invitrogen), which were incubated overnight at 4°C with appropriate primary antibodies: anti-APE /ref-1 raised against peptide from human (1:2000, Novusbio, NB100-116), anti-Neil2, raised against peptide from human (1:5000, Abcam, Ab180576), anti-UNG, raised against peptide from human (1:1000, Abcam, Ab47680), anti-Ogg1, raised against peptide from mouse (1:1000, Novusbio, NB100-61664), respectively. Thereafter, membranes were incubated with appropriate secondary antibody for 1 h at room temperature. Specific proteins were visualized by using the enhanced chemiluminescence procedure using ECL plus® (GE Healthcare, Amersham). All Western blots were run as three replicates, but we have included only a representative image in each figure.

Protein carbonylation

Oxidative modifications of mitochondrial proteins were assessed by immunoblot detection of protein carbonyl groups using the 'OxyBlot' protein oxidation kit according to manufacturer's specifications (Millipore, Chemicon). 10 µg of mitochondrial protein were loaded onto 12.5% SDS-polyacrylamide gel electrophoresis and electrophoretically separated. After the transfer, PVFD membranes were blocked with 1% BSA (in Tris Buffered Saline (TBS) with 0.2% Tween-20) and incubated with anti-dinitrophenylhydrazone antibody, purchased from Chemicon Oxyblot (1:150 working dilution) overnight at 4°C. Thereafter, membranes were incubated with a secondary antibody (goat anti-rabbit IgG (HRP-conjugated)) diluted 1:300 in the blocking solution for 1 h at room temperature. Specific proteins were visualized by using the enhanced chemiluminescence (ECL plus®) procedure as specified by the manufacturer (GE Healthcare, Amersham) and quantified by densitometry using a BioRad scanning densitometer (Bio-Rad, Hercules, CA, USA). The quantification of total protein carbonyls was performed by densitometry of the blots and of the gel stained with Imperial™ Protein Stain (Thermo Scientific), followed by determination of the ratio between them. The samples were run as three replicates, but we have included only a representative image in the figure.

Statistics

Results are expressed as mean ± standard deviation (SD) using three independent mitochondrial preparations. Normality of distribution was checked with the Kolmogorov test, and homogeneity of variance was tested by Levene's statistics. To test for statistically significant differences between the groups, one-way ANOVA was used. When significant F-ratios were observed, a Bonferroni multiple comparison's test was applied to test individual means. Statistical significance was assumed at $P < 0.05$.

Results and Discussion

Mitochondrial DNA glycosylases

The first step in the BER pathway carried out by DNA glycosylases is the recognition and removal of a damaged base and the formation of an AP site (Fig. 1). Since different DNA glycosylases recognize and cleave different DNA lesions, we investigated three DNA glycosylase activities, Neil1/2 glycosylase (Neil1/2), 8-oxoguanine-DNA glycosylase (OGG1) and uracil DNA glycosylase (UNG) known from mammalian mitochondria, using oligonucleotides containing different specific lesions (Table 1). Of these, only the uracil glycosylase activity has been reported for plant mitochondria to date (Bensen and Warner 1987, Boesch et al. 2009).

Neil1/2-like glycosylase in POM

Enzyme activity

In mammals, Neil1 and Neil2 are two glycosylases that repair mainly oxidized DNA lesions and remove oxidized pyrimidines, 2,6-diamino-4-hydroxy-5-formamidopyrimidine and 4,6-diamino-5-formamidopyrimidine, hydroxyuracil, and urea lesions from DNA (Hegde et al. 2008, Hazra et al. 2007, Jaruga et al. 2004, Rosenquist et al. 2003, Wallace et al. 2003). Besides having glycosylase activity both enzymes also have lyase activity (Hazra et al. 2002). In order to characterize the optimal conditions for Neil1/2-like activity in POM, we varied the incubation time, the $MgCl_2$ concentration and the temperature. Neil1/2-like activity increased with incubation time as expected, and showed an optimum activity at 1 mM $MgCl_2$ for both POM and MLM (Fig. 2C, D), under the conditions used. Interestingly, we observed a lower Neil1/2-like activity in POM at 37°C as compared to 25°C (Fig. 2C, D). The Neil1/2-like activity in POM was lower than in MLM, using 25 and 37°C, respectively (Fig. 2D, F).

Immuno-chemistry, proteomics and bioinformatics

A monoclonal antibody raised against human Neil2 (Table 2) was used in Western blots to probe POM for the presence of a protein immunologically similar to Neil 2. It gave a very clear band on a Western blot at the same apparent size of 45 kDa for both MLM and POM (Fig. 2A).

Salvato (2014) identified 1060 different proteins in POM, but there were no glycosylases among them. As the plant mitochondrial proteome is expected to contain 2000-3000 proteins, it was clear that many low-abundance proteins had escaped detection in that study. We therefore performed an in-depth proteomic analysis of POM using a more sensitive mass spectrometer (Supplementary data 7) and identified about 2600 different proteins, many of which were clearly low-abundance proteins. However, none of the identified proteins were annotated as Neil or formamidopyrimidine-DNA glycosylase.

When we searched the full potato protein database we found two proteins annotated as formamidopyrimidine-DNA glycosylase-like proteins and one of them (28 kDa) gave a significant hit to Neil1 (390 amino acids, 44 kDa) with 28% identity over about half of its length) when blasted against the human proteome (Supplementary data 1). This protein has the right size to cross-react with the anti-Neil2 antibody and give the band at 45 kDa.

OGG1-like glycosylase in POM

Enzyme activity

OGG1 catalyzes the excision of 8-oxo-2'-deoxyguanosine (8-Oxo-dG), one of the most common oxidative DNA modifications (Dizdaroglu 1985, Kasai et al. 1986a, Kasai and Nishimura 1986b, Abu-

Shakra and Zeiger 1997, Cadet et al. 2003) in mammalian mitochondria (Anson et al. 1998, LeDoux et al. 1992, Taffe et al. 1996).

When we tried to characterize OGG1-like glycosylase activity in POM, even with a high amount (55 □g) of mitochondria, we were only able to obtain 5% cleavage of the 8-Oxo-dG substrate at 10 mM $MgCl_2$ (Fig. 3C. D). No activity was detected, using different concentrations of $MgCl_2$, even with 1 mM $MgCl_2$, which is normally used in the standard mammalian OGG1 glycosylase activity assay (Gredilla and Stevnsner 2012) or at different temperatures (data not shown). By comparison, 60% substrate conversion was observed using only 30 µg MLM (Fig. 3C, D).

Immuno-chemistry, proteomics and bioinformatics

A polyclonal antibody raised against mouse OGG1 (Table 2) was used in Western blots to probe POM for the presence of a protein immunologically similar to OGG1. It gave a very clear band on a Western blot at 50 kDa in POM as compared to the expected approx. 40 kDa in MLM (Fig. 3A).

Two annotated OGG1 enzymes of approx. 40 and 45 kDa were found in the potato protein database, but not in the in-depth proteome analysis (Supplementary data 2). One was a truncated form of the other. They both showed 39% identity to a mouse oxoguanine DNA glycosylase of about 40 kDa. The larger of these OGG1 enzymes could have given rise to the cross-reactivity in POM on the Western blot.

The in-depth proteomic profiling indentified two DNA glycosylases of 43 and 52 kDa, where one is a truncated version of the other. Both show very significant similarity to a group of rodent adenine DNA glycosylases (Table S1, Supplementary data 2), which can remove 8-Oxo-dG (Ide and Kotera 2004, Alseth et al. 2005). These two glycosylases could therefore also be responsible for the low OGG1-like enzyme activity observed.

UNG1-like glycosylase in POM

Enzyme activity

The last POM glycosylase that we investigated was UNG1 that excises uracil residues from DNA (Fig. 4B, C). UNG1-like glysosylase activity was observed in POM with an optimum at 10 mM $MgCl_2$ (Fig. 4C, D), which is much higher than the 1 mM used in the standard MLM enzyme assay (Gredilla and Stevnsner 2012). It should be noted that the amount of POM used in the assays was 6 times higher than for MLM, but gave similar conversion (Fig. 4C, D), indicating that the activity of UNG1 was much higher in MLM.

Immuno-chemistry, proteomics and bioinformatics

A polyclonal antibody raised against human UNG1 was used in Western blots to probe POM for the presence of a protein immunologically similar to UNG1 in MLM (Fig. 4A). The antibody reacted with proteins migrating at the size of 40, 50 and 110 kDa in POM, where the 110 kDa band was very strong. In MLM, the antibody cross-reacted with a protein of 37 kDa, the expected size.

The in-depth proteomic analysis of POM did not identify any proteins annotated as uracil DNA glycosylases. The potato protein database contains two uracil DNA glycosylases of 30 and 35 kDa. When these were blasted against the human protein database they showed a high degree of similarity to human UNG1 (Supplementary data 3). It is likely that one of these two UNG1-like proteins was responsible for the lowest band on the Western blot in the lane loaded with POM. We do not have any explanation for the other two bands, particularly not the very strongly cross-reacting band at 110 kDa.

Characterization of APE-like activity in POM

Enzyme activity

After monofunctional DNA glycosylases have removed the damaged base in mammalian mtDNA, the endonuclease APE1 cleaves the phosphodiester bond 5′ to give the AP site sugar, generating a nick with 5′ sugar phosphate and 3′ hydroxyl group (Fig. 1).

To characterize the conditions for APE1-like activity in POM, we initially assayed it under the optimal conditions used for MLM. Although the presence of 5 mM $MgCl_2$ improved the efficiency of APE1 activity in MLM, it was not an essential requirement for MLM (data not shown). By contrast, we did not observe APE1 activity in POM in the absence of a metal cofactor (Figs 5C and S1 lanes 2 in panels A, B and C). Likewise, APE1 activity in extracts of *E. coli*, human, and *A. thaliana* is dependent on the presence of divalent cations (Rogers 1980, Kane and Linn 1981, Babiychuk et al. 1994). We therefore examined APE1-like activity in POM in the presence of several different divalent cations and under three different conditions: without any chelating agent, in presence of EDTA (a general divalent cation chelator) or in the presence of EGTA (chelates Ca^{2+} much better than Mg^{2+}). Interestingly, the reaction was much more efficient in the presence of EDTA. APE1-like activity in POM increased with increasing concentration of $MgCl_2$ and $CaCl_2$ up to 10 mM. The combination of EDTA with $MgCl_2$ instead of $CaCl_2$ gave the most efficient cleavage (Figure 5 and Figure S1, panel A, lanes 3 to 7 versus 8 to 12). We also saw that when we substituted EDTA with EGTA, it resulted in a dramatic decrease in APE1 activity (Figs 5 and S1, panel B). Actually, the presence of EGTA did not seem to improve the APE-1 like activity in POM (Figs 5 and S1, panel C).

To further characterize the optimal conditions for the APE1-like activity in POM, we investigated the effects of different concentrations of both $MgCl_2$ and EDTA and compared with MLM APE1 activity.

As already mentioned, POM APE1-like activity was highly dependent on $MgCl_2$. When varying the $MgCl_2$ concentration from 1 mM to 17.5 mM we found bell-shaped curves for both kinds of mitochondria. The optimum was at 10-12.5 mM $MgCl_2$ in POM and 5-12.5 mM $MgCl_2$ in MLM depending on the EDTA concentration (Fig. 6 B, D).

The differences in the rates of product formation observed with different concentrations of divalent cations and chelators could have been caused by changes in the stability of the DNA substrate used in the incision assay. To test that, we determined the melting temperature (T_m) (essentially the double-strand stability) of the nucleotide substrates under the same conditions as used in the experiments described above. No significant differences were found in the DNA dissociation temperature with or without divalent cations (10 mM $MgCl_2$ or $CaCl_2$) or with 1 mM EDTA plus 10 mM $MgCl_2$ (Table S2). Only the addition of $CaCl_2$ together with EDTA showed a small, but significant, change in the T_m. Since this change was very small, we conclude that changes in oligonucleotide stability could not give rise to the results obtained with different combinations of divalent cations and chelators.

Enzyme stability and activity are normally strongly affected by temperature and, while mammalian enzymes in vivo operate at a high and constant temperature, this is not the case for plant enzymes, which are completely dependent on the ambient temperature where they grow. Interestingly, the activity of many plant enzymes measured in vitro is often inhibited as the temperature is raised above 40°C (Larkindale 2005, Allakhverdiev et al. 2008, Mittler et al. 2012). In order to investigate whether high temperatures could compromise the ability of the BER pathway to repair oxidatively damaged mtDNA, we tested the effect of different incubation temperatures on the APE1-like activity.

For APE1 activity in MLM, the product formation was linear for 60 min at all three temperatures tested, 13, 25 and 37°C, respectively (Fig. 7B, E). For POM, the rate was linear at the two lowest temperatures, while it appeared to decrease over time at 37°C (Fig. 7A, D. However, for both MLM and POM the highest activity was observed at 37°C, the body temperature of mouse, but an unusually high temperature for a potato tuber (Fig. 7A, B).

When we tested a broader temperature range, APE1-like activity in POM showed a distinct optimum at 37°C and a dramatic decrease above that. At 42°C, the activity was only 20% of that measured at 37°C (Fig. 7C, F). In contrast, APE1 activity in MLM continued increasing up to 42°C, the highest temperature tested. It appears that mtDNA repair is compromised at high temperatures in potato tubers, whereas it continues unaffected in mouse liver. This is important in order to maintain the ability to repair mtDNA, even when infections lead to an increased temperature of the organism (fever).

Immuno-chemistry, proteomics and bioinformatics

A monoclonal antibody raised against human APE1 was used in Western blots to probe POM for the presence of a protein immunologically similar to APE1 in MLM (Fig. 5A). A band was detected at 75 kDa in POM, while a band at an apparent size of 42 kDa was seen in MLM, close to the expected 37 kDa.

In the in-depth POM proteome profiling we found an apurinic endonuclease of 60 kDa, which showed a high degree of similarity to a human APE of 36 kDa (Table S1, Supplementary data 4), which is consistent with the results from the Western blot.

DNA polymerase and DNA ligase in POM

In mammals, DNA Polβ is known to be a key enzyme in the nuclear BER pathway, whereas the DNA polymerase involved in the mitochondrial BER pathway appears to be Polγ. However, recently Polβ was identified as a mitochondrial DNA polymerase involved in mtDNA maintenance and required for mitochondrial homeostasis in cells from several different mammalian species (Sykora et al. 2017, Kaufman and Van Houten 2017). Interestingly, in the parasite *Trypanosoma brucei* a homolog of Polβ was reported to be solely responsible for the repair and replication of mtDNA (Saxowsky et al. 2003). It is still a matter of debate, which 5′-exo/endonucleases are present and participate in the mammalian mitochondrial LP-BER (Longley et al. 1998, Szczesny et al. 2008).

Three mammalian genes encoding DNA ligases, DNA ligase I (LIG1), DNA ligase III (LIG3) and DNA ligase IV (LIG4), have been identified (Krokan and Bjoras 2013) where LIG1 and LIG3 are involved in BER. LIG3 is essential in mitochondria (Gao et al. 2011, Simsek et al. 2011) for repair of certain types of oxidative lesions (Kubota et al. 1996).

It is difficult to measure the activities of DNA polymerase and DNA ligase separately, because DNA intermediates are quite unstable in vitro if not produced immediately before performing the assays. We therefore used a substrate containing d-Uracil (Table 1). The success of the assay depends on the UNG glycosylase activity together with the AP-lyase activity in the extract to produce the substrate for the DNA polymerase and DNA ligase to act on. In other words, the assay requires that all the enzymes in the BER pathway act sequentially. The assay worked very well with MLM as illustrated in Fig. 8B.

The assay apparently also worked with POM as bands were observed where the DNA polymerase and the DNA ligase products were found as expected. However, when POM were incubated with a DNA oligonucleotide identical to the damaged one, but without the deoxyuracil nucleotide, a similar band pattern was observed. Thus, the incorporation and ligation did not seem to be damage dependent. We

suggest that the optimal conditions for the total BER assay could be slightly different for POM than for MLM. Maybe the observation that there is no lower band in the POM lanes means that there is an unspecific incorporation into the hairpin even when there is nothing to repair. Although we could not confirm either the DNA polymerase or the DNA ligase activity in POM by enzymatic assays, the immuno-chemistry, proteomics and bioinformatics, as described below, show that POM do contain both a DNA polymerase and a DNA ligase.

Immuno-chemistry, proteomics and bioinformatics

A polyclonal antibody raised against the 300-334 amino acid peptide from human Polβ was used in Western blots to probe POM for the presence of a protein immunologically similar to Polβ (Fig. 8). It gave a distinct band at 30 kDa in POM as compared to the expected 38 kDa in MLM (Table 2).

The in-depth proteomic analysis of POM identified a DNA polymerase epsilon catalytic subunit A-like, which was highly similar to the homologous enzyme in humans (Table S1, Supplementary data 5). However, it is much too large to explain the band on the Western blot. We found a protein annotated to be a Polβ in the potato protein database, and it showed a significant similarity to human Polβ (Supplementary data 5). However, we do not know whether this 60 kDa protein is responsible for the 35 kDa band in the Western blot.

The potato protein database did not contain any protein annotated as DNA polymerase gamma, and none of the proteins annotated as DNA polymerases aligned with human DNA polymerase gamma. However, that does not completely exclude the annotated DNA polymerases from having a role in BER in POM. The UniProt database of plant proteins contains only two DNA polymerases annotated as gamma, both from Arabidopsis. When their sequence was blasted against plant proteins, enzymes from numerous species matched closely (60-100% identity), but none from potato (results not shown). Thus, it would appear that the potato protein database is incomplete.

The in-depth proteomic analysis of POM gave a firm identification of a predicted DNA ligase I-like protein (Table S1, Supplementary data 6). When this was blasted against the human proteome it gave very significant hits on DNA ligase I and DNA ligase III, where the latter is the most likely mitochondrial isoform in humans (Supplementary data 6).

Activities of the BER enzymes in POM compared with MLM

Although liver tissue has a rate of respiration many-fold higher than that of dormant potato tubers, this is due to the presence of many-fold more mitochondria per g FW of liver. The yield of isolated mitochondria is around 0.5 mg protein g^{-1} FW of mouse liver (Stevnsner, unpublished results) while it

is 0.01 mg protein g^{-1} FW for potato tubers (Havelund 2014). Isolated POM respire as fast or faster per mg protein than isolated liver mitochondria (Havelund 2014), Stevnsner, unpublished results) and as fast or faster than mitochondria isolated from the metabolically more active potato leaves (Svensson et al. 2002, Johansson et al. 2004). Therefore, in vivo the metabolic activity of the individual mitochondrion would be expected to be as high in potato tubers as in liver and so would the rate of ROS production close to the mtDNA and thus the risk of oxidative DNA damage. It is therefore meaningful to compare the in vitro BER activities of POM and MLM measured in vitro.

We calculated the Neil1/2-like, OGG1-like, UNG1-like and APE1-like specific activities measured in vitro under the optimal assay conditions established and expressed them as fmol min^{-1} mg^{-1} mitochondrial protein (Table 3). For each enzyme, the activity was highest in MLM, in some cases only 2-fold while in other cases > 10-fold. From these observations, it is tempting to draw the conclusion that mtDNA repair mechanisms are not as efficient in potato tubers as in mouse liver.

However, the detergent Triton X-100 was used in all activity assays to solubilize the membranes and allow the enzymes located in the mitochondrial matrix to gain access to the relatively large (30-60 nucleotides = 10-20 kDa) synthetic oligonucleotide substrates, which would not be expected to cross the inner membrane at an appreciable rate. Such a solubilization dilutes the matrix proteins > 1000-fold, which could lead to dissociation of loosely associated proteins, such as metabolons, thereby potentially affecting their function. An example of this is the enzyme complex glycine decarboxylase, which is abundant in the matrix of green leaf mitochondria, and which loses activity when the mitochondria are opened (Douce et al. 2001).

Three out of the four BER proteins identified in our in-depth proteomic study have not been identified in previous studies (Table S1; Salvato et al. 2014). This observation, as well as the few peptides identified for each of the proteins, indicates that these proteins are present at very low abundance in the mitochondrial matrix. It would make sense if these low-abundance enzymes of the BER pathway are found in a supercomplex, a metabolon (Srere 1985), which is held together by weak forces in the matrix (or weakly associated with the inside of the inner mitochondrial membrane) and which therefore could dissociate upon dilution. In fact, the nucleoids associated with the inner membrane of mammalian mitochondria contain some of the BER pathway enzymes (Stuart et al. 2005). The DNA polymerase/DNA ligase assay (Fig. 8) indicates that such a complex is still present in MLM after solubilization and dilution, but probably not in POM. It is difficult to predict how dissociation of such a BER complex could affect the activities of the individual enzymes, and it is therefore difficult to judge to what extent the measured rates reflect their in vivo activities. However, a dissociation of such a BER metabolon would almost certainly inhibit the whole pathway activity drastically because the measured activity is now dependent upon chance of the individual low-abundance proteins

encountering the nucleotide intermediates rather than an ordered sequential channeling within the intact metabolon.

So, our conclusion concerning the relative activities of the BER pathway in plants and animals must be modified to be: There are no indications that the BER pathway is more efficient in POM mitochondria than in mammalian mitochondria. The much slower accumulation of mutations in plant mtDNA than in animal mtDNA, is therefore likely to have other explanations than differences in the efficiency of mitochondrial BER mechanisms.

The mitochondrial BER pathway is induced in potato tubers under hypoxia

In mammalian cells, several studies have demonstrated that oxidative stress can modify BER activity. Thus, DNA Polβ can be up-regulated after oxidative stress in vivo (Cabelof et al. 2002), and in vitro studies show induction of mitochondrial UNG (Akbari et al. 2007) and OGG1 expression in nucleus and mitochondria (Preston et al. 2009). In addition, an increase in mitochondrial OGG1 expression in plant roots, and formamidopyrimidine-DNA glycosylase expression in roots and aerial parts, in response to oxidative stress treatment, has been reported (Macovei et al. 2011).

When the oxygen tension in potato tubers falls to 4% (20% when in equilibrium with air), which can occur when potato tubers are growing, respiration is almost 50% inhibited and ATP production even more so (Geigenberger et al. 2000). Under such conditions, the electron transport chain in the mitochondria becomes more reduced and ROS production increases (Møller 2001). This can lead to damage to proteins and DNA (Møller et al. 2007). To provoke similar strong oxidative stress conditions in vivo, we incubated potato tubers in a 0.1/99.9% O_2/N_2 atmosphere for 48 h before returning them to normoxia for 24 h. We did this because most of the oxidative damage is known to occur during re-oxygenation (Hunter 1983, Monk et al. 1987) similar to what happens following ischemia and reperfusion in mammals (Granger et al. 1986, McCord 1986, Beckman et al. 1990).

To assess oxidative damage, we determined protein carbonyls (as a marker or protein oxidation) in POM. Hypoxia caused a significant increase in carbonyl groups in POM from treated tubers (+20%; $P < 0.05$) compared with the control group (Fig. 9), which is a clear indication of oxidative stress (Møller and Kristensen 2004, Møller et al. 2011).

APE1-like endonuclease and UNG1-like glycosylase activities were determined in mitochondria isolated from control potato tubers and tubers exposed to hypoxia. Fig. 10 (panels A and B) shows that hypoxia induced a significant increase in APE1-like activity when using 45 µg of POM protein. Panels C and D show higher, but non-significant, UNG1-like activity in POM from hypoxic tubers compared to control tubers. The induction of BER pathway enzymes by hypoxia is consistent with the role of the

BER pathway in repairing oxidative DNA damage (Jeppesen et al. 2011). An induction of BER pathway enzymes was also observed in mammalian cells under hypoxia (Akbari et al. 2007, Preston et al. 2009), so it is possible that the regulation of BER activity is similar in plant and mammalian mitochondria.

We have no information about the degree to which mtDNA is oxidatively modified by ROS in plant mitochondria. An indirect indication could be the appearance of oxidized DNA-associated proteins. In a comprehensive proteomic study of potato tuber mitochondria (Salvato et al. 2014), five DNA-associated proteins - DNA polymerase zeta catalytic subunit, DnaK-type molecular chaperone hsp70, DNA topoisomerase 1-like, chaperone DnaJ-domain containing protein and DnaJ-like protein - were found to be carbonylated indicating that even under unstressed conditions the mtDNA and its associated proteins are oxidatively challenged. This is consistent with the presence of many carbonylated proteins in the control POM observed in the present study (Fig. 10). Kristensen and coworkers (Kristensen et al. 2004) did not find any DNA-associated carbonylated proteins in a POM matrix fraction exposed to metal-catalyzed oxidation in vitro, but it is likely that DNA-associated proteins were below the detection limit in that fraction, which was produced by sonication and not by detergent solubilization, and analyzed by the relatively insensitive LC-MS/MS methods of 2003.

Conclusions

In conclusion, the results presented above show that enzymes required for all steps in the BER pathway seems to be present in POM. This information has been summarized in Table 4 together with information about the pathway in Aradidopsis. It remains to be determined whether both the short-patch and long-patch BER pathway is present in POM and whether one or more of the involved glycosylases also display lyase activity.

The second conclusion from this study is that the BER pathway in POM responds to oxidative stress. The BER pathway repairs the majority of the DNA lesions produced by ROS. This pathway primarily corrects small base modifications caused by deamination, alkylation, and oxidation (Kim and Wilson 2012). However, there are many other types of DNA damage and therefore many other repair pathways both in the nucleus and mitochondria of mammalian cells (Jeppesen et al. 2011). These pathways also seem to exist in the nucleus of plants and we can expect to find similar and maybe additional pathways in plant mitochondria. Consistent with this prediction, photolyase activity, which can repair UV-induced cyclobutane-pyrimidine dimers, is found in both plant mitochondria and chloroplasts (Takahashi et al. 2011), while this enzyme is not present in mammalian mitochondria (Alexeyev et al. 2013).

Author contributions

I.M.M., T.S. and K.H.H. conceived the original research plans; I.M.M. and T.S. supervised the experiments; B.F. performed most of the experiments with the assistance of A.L.D.M.F., R.G. and J.F.H.; B.F., I.M.M. and T.S. designed the experiments and analyzed the data; B.F., I.M.M. and T.S. conceived the project and wrote the article with contributions from all the authors.

Acknowledgement – This study was supported by a grant from the Danish Council for Independent Research – Natural Science (FNU) to I.M.M.

A.L.D.M.F. was recipient of mobility doctoral fellowships from Brazilian CNPq-CAPES (Program number 204472/2014-8)

REFERENCES

Abu-Shakra A, Zeiger E (1997) Formation of 8-hydroxy-2'-deoxyguanosine following treatment of 2'-deoxyguanosine or DNA by hydrogen peroxide or glutathione. Mutat Res 390 (1-2):45-50

Akbari M, Otterlei M, Pena-Diaz J, Krokan HE (2007) Different organization of base excision repair of uracil in DNA in nuclei and mitochondria and selective upregulation of mitochondrial uracil-DNA glycosylase after oxidative stress. Neuroscience 145 (4):1201-1212. doi:10.1016/j.neuroscience.2006.10.010

Alexeyev M, Shokolenko I, Wilson G, LeDoux S (2013) The maintenance of mitochondrial DNA integrity--critical analysis and update. Cold Spring Harb Perspect Biol 5 (5):a012641. doi:10.1101/cshperspect.a012641

Allakhverdiev SI, Kreslavski VD, Klimov VV, Los DA, Carpentier R, Mohanty P (2008) Heat stress: an overview of molecular responses in photosynthesis. Photosynth Res 98 (1-3):541-550. doi:10.1007/s11120-008-9331-0

Alseth I, Osman F, Korvald H, Tsaneva I, Whitby MC, Seeberg E, Bjoras M (2005) Biochemical characterization and DNA repair pathway interactions of Mag1-mediated base excision repair in Schizosaccharomyces pombe. Nucleic Acids Res 33 (3):1123-1131. doi:10.1093/nar/gki259

Altschul SM, TL.; Schäffer, AA.; Zhang, J.; Zhan, Z.; Miller, W.; and Lipman, DJ. (1997) Gapped BLAST and PSI-BLAST: a new generation of protein database search programs. Nucleic Acids Res 25:3389-3402

Anson RM, Croteau DL, Stierum RH, Filburn C, Parsell R, Bohr VA (1998) Homogenous repair of singlet oxygen-induced DNA damage in differentially transcribed regions and strands of human mitochondrial DNA. Nucleic Acids Res 26 (2):662-668

Babiychuk E, Kushnir S, Vanmontagu M, Inze D (1994) The Arabidopsis-Thaliana Apurinic Endonuclease Arp Reduces Human Transcription Factors Fos and Jun. P Natl Acad Sci USA 91 (8):3299-3303. doi:DOI 10.1073/pnas.91.8.3299

Beckman JS, Beckman TW, Chen J, Marshall PA, Freeman BA (1990) Apparent hydroxyl radical production by peroxynitrite: implications for endothelial injury from nitric oxide and superoxide. Proc Natl Acad Sci U S A 87 (4):1620-1624

Bensen RJ, Warner HR (1987) Partial Purification and Characterization of Uracil-DNA Glycosylase Activity from Chloroplasts of Zea mays Seedlings. Plant Physiol 84 (4):1102-1106

Boesch P, Ibrahim N, Paulus F, Cosset A, Tarasenko V, Dietrich A (2009) Plant mitochondria possess a short-patch base excision DNA repair pathway. Nucleic Acids Res 37 (17):5690-5700. doi:10.1093/nar/gkp606

Bradford MM (1976) A rapid and sensitive method for the quantitation of microgram quantities of protein utilizing the principle of protein-dye binding. Anal Biochem 72:248-254

Cabelof DC, Raffoul JJ, Yanamadala S, Guo Z, Heydari AR (2002) Induction of DNA polymerase beta-dependent base excision repair in response to oxidative stress in vivo. Carcinogenesis 23 (9):1419-1425

Cadet J, Douki T, Gasparutto D, Ravanat JL (2003) Oxidative damage to DNA: formation, measurement and biochemical features. Mutat Res 531 (1-2):5-23

Cordoba-Canero D, Roldan-Arjona T, Ariza RR (2014) Arabidopsis ZDP DNA 3'-phosphatase and ARP endonuclease function in 8-oxoG repair initiated by FPG and OGG1 DNA glycosylases. Plant J 79 (5):824-834. doi:10.1111/tpj.12588

Dizdaroglu M (1985) Formation of an 8-hydroxyguanine moiety in deoxyribonucleic acid on gamma-irradiation in aqueous solution. Biochemistry 24 (16):4476-4481

Douce R, Bourguignon J, Neuburger M, Rebeille F (2001) The glycine decarboxylase system: a fascinating complex. Trends Plant Sci 6 (4):167-176. doi:Doi 10.1016/S1360-1385(01)01892-1

Foyer CH, Noctor G (2003) Redox sensing and signalling associated with reactive oxygen in chloroplasts, peroxisomes and mitochondria. Physiologia Plantarum 119 (3):355-364. doi:DOI 10.1034/j.1399-3054.2003.00223.x

Gao Y, Katyal S, Lee Y, Zhao J, Rehg JE, Russell HR, McKinnon PJ (2011) DNA ligase III is critical for mtDNA integrity but not Xrcc1-mediated nuclear DNA repair. Nature 471 (7337):240-244. doi:10.1038/nature09773

Geigenberger P, Fernie AR, Gibon Y, Christ M, Stitt M (2000) Metabolic activity decreases as an adaptive response to low internal oxygen in growing potato tubers. Biol Chem 381 (8):723-740. doi:10.1515/BC.2000.093

Granger DN, Hollwarth ME, Parks DA (1986) Ischemia-reperfusion injury: role of oxygen-derived free radicals. Acta Physiol Scand Suppl 548:47-63

Gredilla R, Stevnsner T (2012) Mitochondrial base excision repair assays. Methods Mol Biol 920:289-304. doi:10.1007/978-1-61779-998-3_20

Grollman AP, Moriya M (1993) Mutagenesis by 8-Oxoguanine - an Enemy Within. Trends Genet 9 (7):246-249. doi:Doi 10.1016/0168-9525(93)90089-Z

Gualberto JM, Newton KJ (2017) Plant Mitochondrial Genomes: Dynamics and Mechanisms of Mutation. Annu Rev Plant Biol 68:225-252. doi:10.1146/annurev-arplant-043015-112232

Havelund JF, Salvato, F., Chen, M., Rao, R.S.P., Wrzesinska-Rogowska, A., Jensen, O.N., Gang, D.R., Thelen, J.J., Møller, I.M. (2014) Isolation of potato tuber mitochondria. . Bio-protocol 4(17): e1226

Hazra TK, Das A, Das S, Choudhury S, Kow YW, Roy R (2007) Oxidative DNA damage repair in mammalian cells: a new perspective. DNA Repair (Amst) 6 (4):470-480. doi:10.1016/j.dnarep.2006.10.011

Hazra TK, Izumi T, Boldogh I, Imhoff B, Kow YW, Jaruga P, Dizdaroglu M, Mitra S (2002) Identification and characterization of a human DNA glycosylase for repair of modified bases in oxidatively damaged DNA. Proc Natl Acad Sci U S A 99 (6):3523-3528. doi:10.1073/pnas.062053799

Hegde ML, Hazra TK, Mitra S (2008) Early steps in the DNA base excision/single-strand interruption repair pathway in mammalian cells. Cell Res 18 (1):27-47. doi:10.1038/cr.2008.8

Hunter MISH, A.M.; Crawford, R.M.M. (1983) Lipid peroxidation—a factor in anoxia intolerance in Iris species. Phytochemistry, 22:1145–1147.

Ide H, Kotera M (2004) Human DNA glycosylases involved in the repair of oxidatively damaged DNA. Biol Pharm Bull 27 (4):480-485

Jaruga P, Birincioglu M, Rosenquist TA, Dizdaroglu M (2004) Mouse NEIL1 protein is specific for excision of 2,6-diamino-4-hydroxy-5-formamidopyrimidine and 4,6-diamino-5-formamidopyrimidine from oxidatively damaged DNA. Biochemistry 43 (50):15909-15914. doi:10.1021/bi048162l

Jeppesen DK, Bohr VA, Stevnsner T (2011) DNA repair deficiency in neurodegeneration. Prog Neurobiol 94 (2):166-200. doi:10.1016/j.pneurobio.2011.04.013

Johansson FI, Michalecka AM, Moller IM, Rasmusson AG (2004) Oxidation and reduction of pyridine nucleotides in alamethicin-permeabilized plant mitochondria. Biochem J 380 (Pt 1):193-202. doi:10.1042/BJ20031969

Kane CM, Linn S (1981) Purification and Characterization of an Apurinic-Apyrimidinic Endonuclease from Hela-Cells. J Biol Chem 256 (7):3405-3414

Kasai H, Crain PF, Kuchino Y, Nishimura S, Ootsuyama A, Tanooka H (1986a) Formation of 8-hydroxyguanine moiety in cellular DNA by agents producing oxygen radicals and evidence for its repair. Carcinogenesis 7 (11):1849-1851

Kasai H, Nishimura S (1986b) Hydroxylation of guanine in nucleosides and DNA at the C-8 position by heated glucose and oxygen radical-forming agents. Environ Health Perspect 67:111-116

Kaufman BA, Van Houten B (2017) POLB: A new role of DNA polymerase beta in mitochondrial base excision repair. DNA Repair (Amst) 60:A1-A5. doi:10.1016/j.dnarep.2017.11.002

Kavli B, Otterlei M, Slupphaug G, Krokan HE (2007) Uracil in DNA-general mutagen, but normal intermediate in acquired immunity. DNA Repair 6 (4):505-516. doi:10.1016/j.dnarep.2006.10.014

Kazak L, Reyes A, Holt IJ (2012) Minimizing the damage: repair pathways keep mitochondrial DNA intact. Nat Rev Mol Cell Biol 13 (10):659-671. doi:10.1038/nrm3439

Kim YJ, Wilson DM, 3rd (2012) Overview of base excision repair biochemistry. Curr Mol Pharmacol 5 (1):3-13

Kristensen BK, Askerlund P, Bykova NV, Egsgaard H, Moller IM (2004) Identification of oxidised proteins in the matrix of rice leaf mitochondria by immunoprecipitation and two-dimensional

liquid chromatography-tandem mass spectrometry. Phytochemistry 65 (12):1839-1851. doi:10.1016/j.phytochem.2004.04.007

Krokan HE, Bjoras M (2013) Base excision repair. Cold Spring Harb Perspect Biol 5 (4):a012583. doi:10.1101/cshperspect.a012583

Kubota Y, Nash RA, Klungland A, Schar P, Barnes DE, Lindahl T (1996) Reconstitution of DNA base excision-repair with purified human proteins: interaction between DNA polymerase beta and the XRCC1 protein. EMBO J 15 (23):6662-6670

Larkindale J, Mishkind, M., Vierling, E. (2005) Plant responses to high temperature. In: Plant Abiotic Stress Ed MA Jenks, PM Hasegawa:100-144

LeDoux SP, Wilson GL, Beecham EJ, Stevnsner T, Wassermann K, Bohr VA (1992) Repair of mitochondrial DNA after various types of DNA damage in Chinese hamster ovary cells. Carcinogenesis 13 (11):1967-1973

Liu BY, Xue QZ, Tang Y, Cao J, Guengerich FP, Zhang HD (2016) Mechanisms of mutagenesis: DNA replication in the presence of DNA damage. Mutat Res-Rev Mutat 768:53-67. doi:10.1016/j.mrrev.2016.03.006

Longley MJ, Prasad R, Srivastava DK, Wilson SH, Copeland WC (1998) Identification of 5'-deoxyribose phosphate lyase activity in human DNA polymerase gamma and its role in mitochondrial base excision repair in vitro. Proc Natl Acad Sci U S A 95 (21):12244-12248

Lynch M (2007) The origins of genome achitecture. Sunderland (MA): Sinauer Associates, Inc 2007

Lynch M, Koskella B, Schaack S (2006) Mutation pressure and the evolution of organelle genomic architecture. Science 311 (5768):1727-1730. doi:10.1126/science.1118884

Macovei A, Balestrazzi A, Confalonieri M, Fae M, Carbonera D (2011) New insights on the barrel medic MtOGG1 and MtFPG functions in relation to oxidative stress response in planta and during seed imbibition. Plant Physiol Biochem 49 (9):1040-1050. doi:10.1016/j.plaphy.2011.05.007

Maxwell DP, Wang Y, McIntosh L (1999) The alternative oxidase lowers mitochondrial reactive oxygen production in plant cells. P Natl Acad Sci USA 96 (14):8271-8276. doi:DOI 10.1073/pnas.96.14.8271

Maynard S, Schurman SH, Harboe C, de Souza-Pinto NC, Bohr VA (2009) Base excision repair of oxidative DNA damage and association with cancer and aging. Carcinogenesis 30 (1):2-10. doi:10.1093/carcin/bgn250

McCord JM (1986) Superoxide dismutase: rationale for use in reperfusion injury and inflammation. J Free Radic Biol Med 2:307-310

Mittler R, Finka A, Goloubinoff P (2012) How do plants feel the heat? Trends Biochem Sci 37 (3):118-125. doi:10.1016/j.tibs.2011.11.007

Møller IM (2001) Plant mitochondria and oxidative stress: Electron transport, NADPH turnover, and metabolism of reactive oxygen species. Annu Rev Plant Phys 52:561-591. doi:DOI 10.1146/annurev.arplant.52.1.561

Møller IM, Jensen PE, Hansson A (2007) Oxidative modifications to cellular components in plants. Annu Rev Plant Biol 58:459-481. doi:10.1146/annurev.arplant.58.032806.103946

Møller IM, Kristensen BK (2004) Protein oxidation in plant mitochondria as a stress indicator. Photochem Photobiol Sci 3 (8):730-735. doi:10.1039/b315561g

Møller IM, Rogowska-Wrzesinska A, Rao RS (2011) Protein carbonylation and metal-catalyzed protein oxidation in a cellular perspective. J Proteomics 74 (11):2228-2242. doi:10.1016/j.jprot.2011.05.004

Monk LS, Fagerstedt KV, Crawford RM (1987) Superoxide Dismutase as an Anaerobic Polypeptide : A Key Factor in Recovery from Oxygen Deprivation in Iris pseudacorus? Plant Physiol 85 (4):1016-1020

Oldenburg DJ, Bendich AJ (2015) DNA maintenance in plastids and mitochondria of plants. Front Plant Sci 6. doi:ARTN 883

10.3389/fpls.2015.00883

Palmer JD, Herbon LA (1988) Plant mitochondrial DNA evolves rapidly in structure, but slowly in sequence. J Mol Evol 28 (1-2):87-97

Prasad R, Caglayan M, Dai DP, Nadalutti CA, Zhao ML, Gassman NR, Janoshazi AK, Stefanick DF, Horton JK, Krasich R, Longley MJ, Copeland WC, Griffith JD, Wilson SH (2017) DNA polymerase beta: A missing link of the base excision repair machinery in mammalian mitochondria. DNA Repair (Amst) 60:77-88. doi:10.1016/j.dnarep.2017.10.011

Preston TJ, Henderson JT, McCallum GP, Wells PG (2009) Base excision repair of reactive oxygen species-initiated 7,8-dihydro-8-oxo-2'-deoxyguanosine inhibits the cytotoxicity of platinum anticancer drugs. Mol Cancer Ther 8 (7):2015-2026. doi:10.1158/1535-7163.MCT-08-0929

Rogers SW, B. (1980) Exonuclease III of Escherichia coli K-12, an AP endonuclease. . Methods Enzymol 65:201–211

Rosenquist TA, Zaika E, Fernandes AS, Zharkov DO, Miller H, Grollman AP (2003) The novel DNA glycosylase, NEIL1, protects mammalian cells from radiation-mediated cell death. DNA Repair (Amst) 2 (5):581-591

Salvato F, Havelund JF, Chen M, Rao RS, Rogowska-Wrzesinska A, Jensen O, Gang D, Thelen J, Moller I (2014) The potato tuber mitochondrial proteome. Plant Physiol 164 (2):637-653. doi:10.1104/pp.113.229054

Saxowsky TT, Choudhary G, Klingbeil MM, Englund PT (2003) Trypanosoma brucei has two distinct mitochondrial DNA polymerase beta enzymes. J Biol Chem 278 (49):49095-49101. doi:10.1074/jbc.M308565200

Simsek D, Furda A, Gao Y, Artus J, Brunet E, Hadjantonakis AK, Van Houten B, Shuman S, McKinnon PJ, Jasin M (2011) Crucial role for DNA ligase III in mitochondria but not in Xrcc1-dependent repair. Nature 471 (7337):245-248. doi:10.1038/nature09794

Srere PA (1985) The metabolon. . Trends Biochem Sci 10(3):109–110

Stuart JA, Mayard S, Hashiguchi K, Souza-Pinto NC, Bohr VA (2005) Localization of mitochondrial DNA base excision repair to an inner membrane-associated particulate fraction. Nucleic Acids Res 33 (12):3722-3732. doi:10.1093/nar/gki683

Sunderland PA, West CE, Waterworth WM, Bray CM (2006) An evolutionarily conserved translation initiation mechanism regulates nuclear or mitochondrial targeting of DNA ligase 1 in Arabidopsis thaliana. Plant J 47 (3):356-367. doi:10.1111/j.1365-313X.2006.02791.x

Svensson AS, Johansson FI, Moller IM, Rasmusson AG (2002) Cold stress decreases the capacity for respiratory NADH oxidation in potato leaves. FEBS Lett 517 (1-3):79-82

Sykora P, Kanno S, Akbari M, Kulikowicz T, Baptiste BA, Leandro GS, Lu H, Tian J, May A, Becker KA, Croteau DL, Wilson DM, 3rd, Sobol RW, Yasui A, Bohr VA (2017) DNA polymerase beta participates in mitochondrial DNA repair. Mol Cell Biol. doi:10.1128/MCB.00237-17

Szczesny B, Tann AW, Longley MJ, Copeland WC, Mitra S (2008) Long patch base excision repair in mammalian mitochondrial genomes. J Biol Chem 283 (39):26349-26356. doi:10.1074/jbc.M803491200

Taffe BG, Larminat F, Laval J, Croteau DL, Anson RM, Bohr VA (1996) Gene-specific nuclear and mitochondrial repair of formamidopyrimidine DNA glycosylase-sensitive sites in Chinese hamster ovary cells. Mutat Res 364 (3):183-192

Takahashi M, Teranishi M, Ishida H, Kawasaki J, Takeuchi A, Yamaya T, Watanabe M, Makino A, Hidema J (2011) Cyclobutane pyrimidine dimer (CPD) photolyase repairs ultraviolet-B-induced CPDs in rice chloroplast and mitochondrial DNA. Plant J 66 (3):433-442. doi:10.1111/j.1365-313X.2011.04500.x

Trasvina-Arenas CH, Baruch-Torres N, Cordoba-Andrade FJ, Ayala-Garcia VM, Garcia-Medel PL, Diaz-Quezada C, Peralta-Castro A, Ordaz-Ortiz JJ, Brieba LG (2018) Identification of a unique insertion in plant organellar DNA polymerases responsible for 5'-dRP lyase and strand-displacement activities: Implications for Base Excision Repair. DNA Repair (Amst) 65:1-10. doi:10.1016/j.dnarep.2018.02.010

Wallace SS, Bandaru V, Kathe SD, Bond JP (2003) The enigma of endonuclease VIII. DNA Repair (Amst) 2 (5):441-453

Supporting information

Table S1. BER proteins identified in POM by in-depth proteomic profiling.

Table S2. DNA melting temperature.

Fig. S1. Effects of the concentration of divalent cations ($MgCl_2$ or $CaCl_2$) and/or presence of 1 mM EDTA or EGTA in the reaction buffer on the POM AP endonuclease activity.

Supplementary data 1. Neil1/2-like glycosylase

Supplementary data 2. OGG1-like glycosylase

Supplementary data 3. UNG1-like glycosylase

Supplementary data 4. Apurinic endonuclease

Supplementary data 5. DNA polymerase

Supplementary data 6. DNA ligase

Supplementary data 7. Proteomic profiling of POM method

FIGURE LEGENDS

Fig. 1. Schematic drawing of the BER pathway.

Fig. 2. Effects of the concentration of $MgCl_2$ on the MLM and POM Neil1/2 glycosylase activity. (A) Representative western blot of Neil1/2 in POM and MLM. (B) 5-OH-dU bubble substrate used for incision experiment. (C). 36 fmol 5'- 32P-labelled 5-OH-dU bubble substrate was incubated with different concentrations of $MgCl_2$ at conditions indicated under glycosylases incision assay conditions. (D) Densitometric quantification of autoradiogram shown in (C). (E) 36 fmol 5'- 32P-labelled 5-OH-dU bubble substrate was incubated with 30 µg of MLM or POM, as indicated, for 180 min at conditions described under glycosylases incision assay protocol. (F) Densitometric quantification of autoradiogram shown in (E).

Fig. 3. Identification of OGG1 glysosylase. (A) Representative western blot of OGG1 in POM and MLM. (B) 8-Oxo-dG substrate in fully annealed DNA used for incision experiment. (C) 80 fmol 5'- 32P-labelled 8-Oxo-dG substrate was incubated in 10 mM $MgCl_2$ for POM and 1 mM $MgCl_2$ for MLM under glycosylases incision assay condition. (D) Densitometric quantification of autoradiogram in (C).

Fig. 4. Effects of the concentration of $MgCl_2$ on the MLM and POM UNG1 glycosylase activity. (A) Representative western blot of UNG1 POM and MLM. (B) Uracil substrate in fully annealed DNA used for incision experiment. (C) 36 fmol 5'- 32P-labelled uracil substrate was incubated with different concentrations of $MgCl_2$ in the indicated conditions under glycosylases incision assay condition. (D) Densitometric quantification of autoradiogram shown in (C).

Fig. 5. AP endonuclease characterization in POM. (A) Representative western blot of APE1 in POM and MLM. (B) THF substrate in fully annealed DNA used for incision experiment. (C) Divalent cation concentration dependence ($MgCl_2$ or $CaCl_2$) of APE1 activity with or without 1 mM EDTA or 1 mM EGTA. For the incision assay 36 fmol 5'- 32P-labelled THF substrate was incubated for 30 min at 25°C with 6 µg POM protein under APE1 incision assay conditions.

Fig. 6. Effects of the concentration of $MgCl_2$ with different concentrations of EDTA in the reaction buffer on the MLM and POM AP endonuclease activity. For the incision assay 36 fmol 5'- 32P-labelled THF substrate was incubated for 30 min at 37°C with 0.1 µg MLM protein (A), and 25°C with 0.2 µg POM protein (B) under APE1 incision assay conditions and with different concentrations of EDTA and $MgCl_2$. Panels (C) and (D) Densitometric quantification of autoradiogram shown in (A) and (B), respectively.

Fig. 7. Effects of different incubation temperatures and increasing incubation time on the MLM and POM AP endonuclease activity. Panels (A) to (C) show 36 fmol 5'- 32P-labelled THF substrate incubated with the indicated conditions under APE1 incision assay protocol. Panels (D) to (F) Densitometric quantification of autoradiogram shown in (A), (B) and (C), respectively.

Fig. 8. Presence of Polβ protein in the POM. (A) Representative western blot of Polβ in MLM and POM. (B) Uracil-initiated BER. Non-labeled 60 base-pair hairpin loop oligonucleotide with or without a d-Uracil was incubated with the indicated conditions DNA polymerase and DNA ligase activity assay protocol. (Lanes 4 and 5 are duplicates for MLM and lanes 7 and 8 are duplicates for POM).

Fig. 9. Hypoxic treatment induces oxidative stress in POM. (A) Representative western blot of carbonylated POM proteins. (B) Gel stained with coomassie blue G250 was used as a loading control. (C) Ratio between densitometric quantification using relative expression in arbitrary units of carbonylated proteins and coomassie blue staining for normoxic (N) and, hypoxic (H) POM. Results are expressed as means ± SD. of triplicate measurements from three independent mitochondrial treatment preparations. A two-factor ANOVA and post hoc Bonferroni's comparisons were used to identify significant differences.

Fig. 10. Effects of the hypoxic treatment on POM on BER activities. Representative gels of APE1 (A) and UNG1 (B) activities for hypoxic (H) and normoxic (N) POM, on BER optimal conditions at 25°C. Quantified product cleavage for APE1 activity (C) and UNG1 activity (D), expressed as means ± SD. of triplicate measurements from three independent mitochondrial treatment preparations. An one-factor ANOVA and post hoc Bonferroni's comparisons were used to identify significant differences. *difference hypoxic vs normoxic treatment ($P < 0.05$).

Table 1. Oligonucleotide sequences in assays for DNA repair activities. Oligodeoxynucleotides used for assays for DNA repair activities. The modified bases are shown in bold X letter. The region forming a bubble sequence is underlined. Bp, base pairs. THF, tetrahydrofuran.

Name	Enzyme	bp	Sequence	
5-OH-dU bubble	Neil 1/2	51	5′-GCTTAGCTTGGAATCGTATCATGTAXACTCGTGTGCCGTGTAGACCGTGCC-3′	X=5-OH-dU
			3′-CGAATCGAACCTTAGCATAGTACATGTGAGCACACGGCACATCTGGCACGG-5′	
8-Oxo-dG	OGG1	30	5′-ATATACCGCGXCCGGCCGATCAAGCTTATT-3′	X=8-Oxo-dG
			3′-TATATGGCGCCGGCCGGCTAGTTCGAATAA-5′	
Uracil	Uracil glycosylase	30	5′-ATATACCGCGGXCGGCCGATCAAGCTTATT-3′	X=dU
			3′-TATATGGCGCCGGCCGGCTAGTTCGAATAA-5′	
THF (AP-site analogue)	APE 1	30	5′-ATATACCGCGGXCGGCCGATCAAGCTTATT-3′	X=THF
			3′-TATATGGCGCCGGCCGGCTAGTTCGAATAA-5′	
dU-BER (harpin loop)	Whole BER pathway	60	5'-ATATACCACGTCGGXGATCCAGTCCTGCTTTTGCAGGACTGGATCGCCGACGTGGTATAT-3'	X=dU

Table 2. Antibodies used to identify BER pathway enzymes in POM and MLM.

Antibody	Reference	Clonality	Dilution	Size (kDa)		
				Expected	POM	MLM
Human Neil2	Abcam 180576	Monoclonal	1:5000	37	45	45
Mouse OGG1	NovusBio 100-61664	Polyclonal	1:5000	39	50	40
Human UNG1	Abcam 47680	Polyclonal	1:1000	37	110-50-40	37
Human APE	NovusBio 100-116	Monoclonal	1:2000	37	75	42
Human Polβ	Abcam 26343	Polyclonal	1:5000	35	31	38

Table 3. POM enzymes activities and conditions compared with MLM. Values for AP endonuclease and DNA glycosylase activities in mitochondria from POM and MLM, expressed as fmol per minute per µg of mitochondria, and the different conditions used for optimal incision assay activity at 25 °C and 37 °C for POM and MLM, respectively.

Substrate	Sample	Temperature (°C)	$MgCl_2$ (mM)	EDTA (mM)	fmol product min-1 mg-1 protein
NEIL1/2	POM	25	1	5	1.6
	MLM	37	1	5	3.8
UNG1	POM	25	10	5	2.8
	MLM	37	1	5	7.6
OGG1	POM	25	10	5	0.16
	MLM	37	1	5	4.1
APE1	POM	25	10	1	1020
	MLM	37	5	1	45400

Table 4. Comparison of mitochondrial BER pathway between Arabidopsis thaliana and Solanum tuberosum. FapyG, 2,6-diamino-4-hydroxy-5-formamidopyrimidine. FapyA, 4,6-diamino-5-formamidopyrimidine.

Enzyme	Molecular function	Studied species	Gene identifier	Gene/protein annotation	References
Neil 1/2	Excision of oxidized pyrimidines, FapyG, FapyA, 5-OHU, and urea lesions	*Arabidopsis thaliana*	-	-	-
		Solanum tubersosum	>gi|971540183|ref|XP_015161662.1 >gi|971540185|ref|XP_015161663.1|	Predicted: formamidopyrimidine-DNA glycosylase-like isoform X2 Predicted: formamidopyrimidine-DNA glycosylase-like	This study
OGG1	Excision of 8-Oxo-dG	*Arabidopsis thaliana*	At1g52500	Predicted bifunctional glycosylase	(Cordoba-Canero et al. 2014)
		Solanum tubersosum	>gi|565369036|ref|XP_006351143.1| >gi|565369034|ref|XP_006351142.1| >gi|565354925|ref|XP_006344357.1|	Predicted: N-glycosylase/DNA lyase OGG1 Predicted: N-glycosylase/DNA lyase OGG1 Predicted: A/G-specific adenine DNA glycosylase-like isoform X1	This study
Uracil glycosylase	Excision of uracil residues	*Arabidopsis thaliana*	At3g18630	Predicted monofunctional glycosylase	(Boesch et al. 2009)
		Solanum tubersosum	>gi|971555743|ref|XP_015165515.1| >gi|565367417|ref|XP_006350364.1|	Predicted: uracil-DNA glycosylase, mitochondrial isoform X2 Predicted: uracil-DNA glycosylase, mitochondrial isoform X1	(Boesch et al. 2009); This study

APE1	Creation of a nick in the phosphodiester backbone of the AP site	*Arabidopsis thaliana*	-	Predicted: AP endonuclease activity	(Boesch et al. 2009)
		Solanum tubersosum	>gi|565383436|ref|XP_006358023.1|	Predicted: DNA-(apurinic or apyrimidinic site) lyase, chloroplastic isoform X1	(Boesch et al. 2009); This study
DNA polymerase	Gap filling of the DNA strand	*Arabidopsis thaliana*	-	-	-
		Solanum tubersosum	>gi|565364804|ref|XP_006349108.1| >gi|565379014|ref|XP_006355938.1|	Predicted: DNA polymerase epsilon catalytic subunit A-like Predicted: DNA polymerase beta	This study
DNA ligase	Nick ligation	*Arabidopsis thaliana*	At1g08130 (AtLIG1)	Mitochondrial DNA ligase	(Sunderland et al. 2006)
		Solanum tubersosum	gi|565364649|ref|XP_006349032.1|	Predicted: DNA ligase 1-like	This study

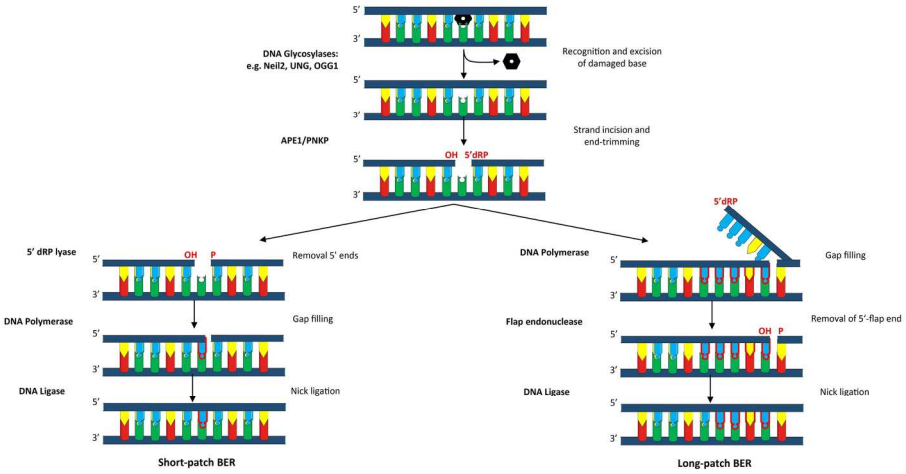

Figure 1

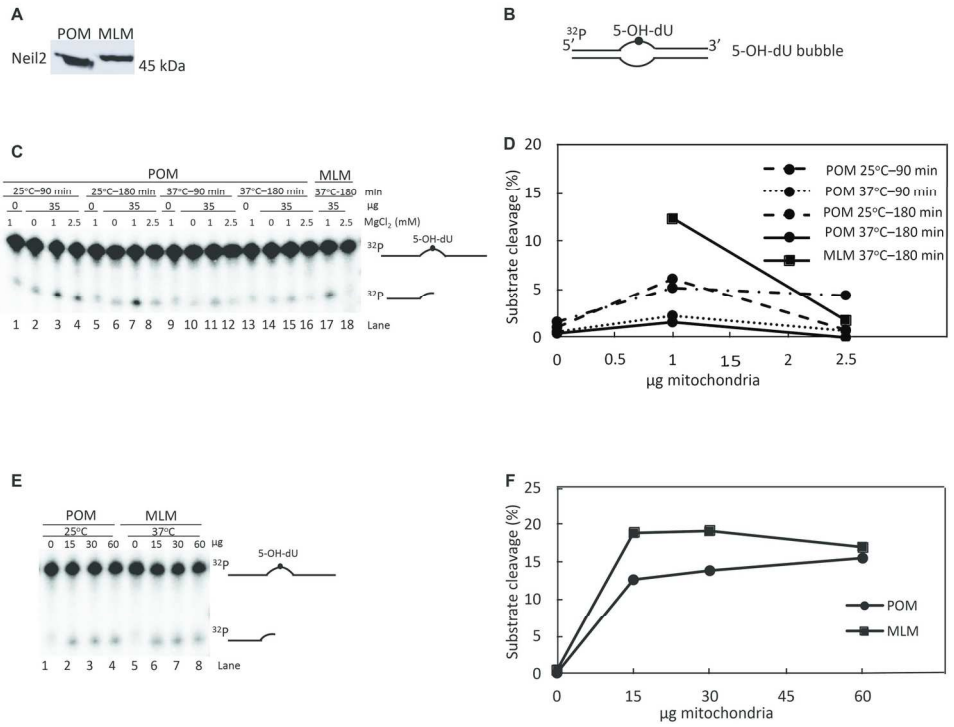

Figure 2

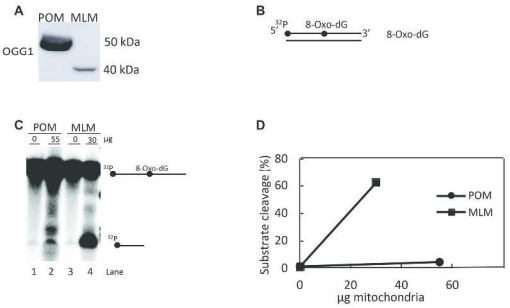

Figure 3

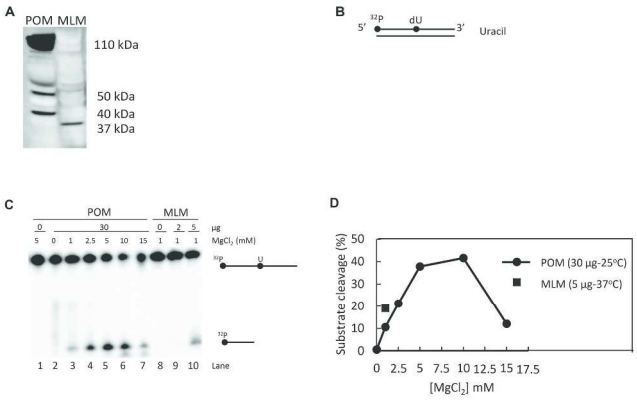

Figure 4

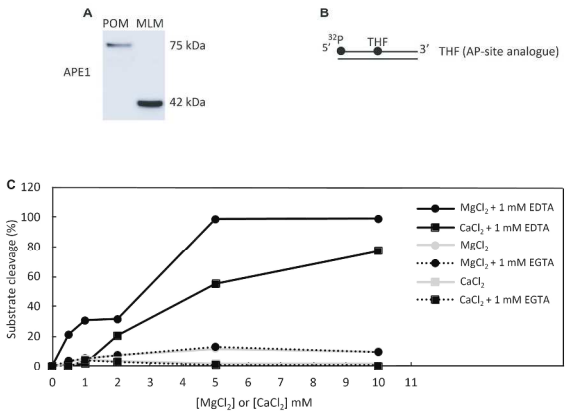

Figure 5

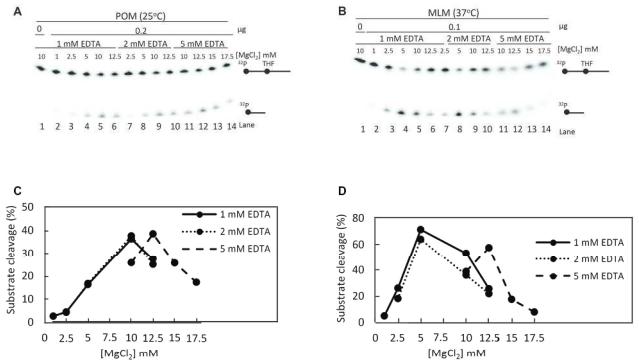

Figure 6

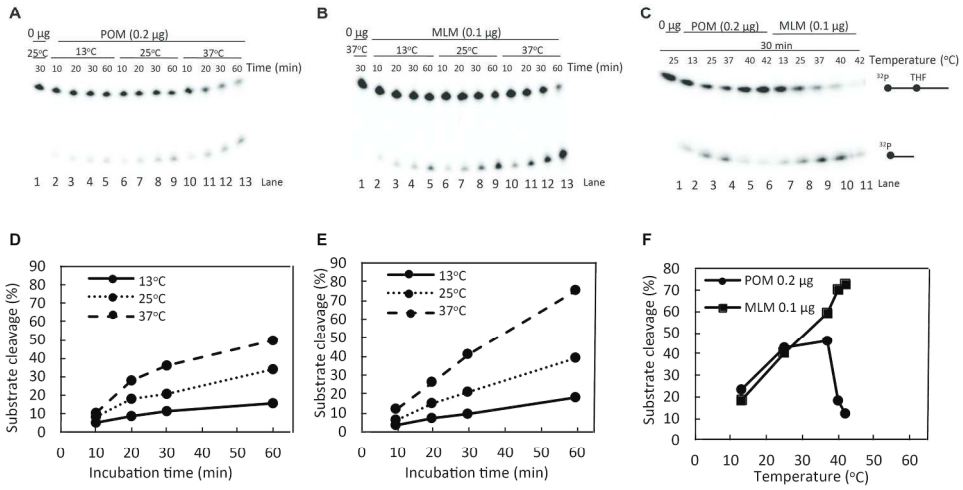

Figure 7

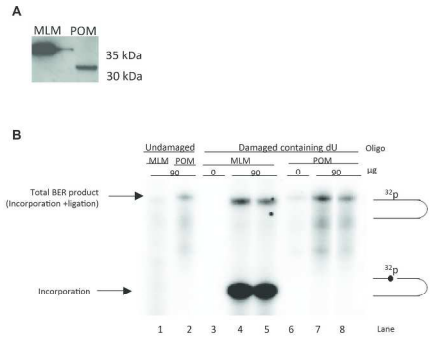

Figure 8

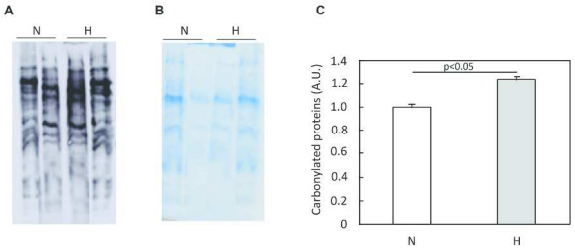

Figure 9

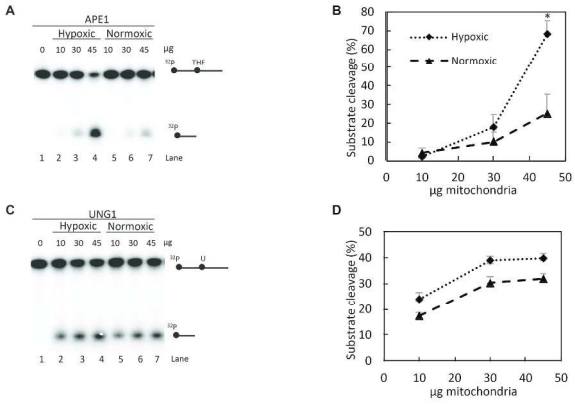

Figure 10